A Vibrating-Dipole Technique for Measuring Millimeter-Wave Fields in Free Space

NEVILLE A. MATHEWS AND HENRYK STACHERA

Abstract—**EM field measuring techniques, based on the modulated-scattering principle, are well established at microwave frequencies. The main difficulty in extending measurements to the millimeter-wave region is that of scaling the scatterer for operation at these wavelengths. The technique of modulated scattering described in this paper overcomes this limitation. A thin metallic dipole, attached to a vibrating nylon cord, forms the modulated scatterer which interacts with the electric field and gives rise to a phase-modulated reflected wave. The reflected wave is then combined with a reference wave in a coherent detection system. The detected signal contains information about the amplitude and phase of the field at the midpoint of the dipole's vibration.**

An analysis of the technique is presented and the factors affecting the accuracy of measurement are fully discussed. It is shown how the measurement errors can be minimized. Amplitude and phase measurements, taken at a wavelength of 4.8 mm, verify the validity and accuracy of the technique.

I. Introduction

THE vibrating-dipole technique was developed as part of a research program on the propagation of EM waves in the 50–75-GHz band. One problem of particular interest was the experimental determination of fields diffracted by apertures and obstacles.

We have first examined the established techniques and found that most conventional methods did not lend themselves to our problem. Techniques involving direct probing [1]–[4] of the field require transmission leads which distort the field. Furthermore, the unavoidable positioning of the transmission line, as the probe is moved to different locations in space, makes phase measurements unreliable. At millimetric wavelengths these effects are particularly severe.

Perturbation techniques, widely used in microwave cavities [5]–[8] and waveguides [9], [10] are free from the transmission-line limitation. The underlying principle is that the field reradiated by the perturbing element is directly related to the electric and/or magnetic field at the location of the scatterer in its absence. A simple perturbation technique can also be used to explore EM fields in free space, but in most applications the scattered signal is too weak to be reliably separated from the background reflections. In an effort to separate the wanted scattered signal, it has been modulated electrically [11], [12], optically [13]–[15], or mechanically [16], [17]. In all these modulated-scattering methods considerable ingenuity has been displayed to reduce the physical size of scatterers. Some scatterers have been successfully scaled down for use in X band [11]–[14] but none would be made sufficiently small for use at shorter millimetric wavelengths. At these wavelengths, particularly difficult to measure are near-fields of diffracting apertures and obstacles. For these applications the scatterer must be electrically small if accurate measurements of amplitude and phase are to be made. At a wavelength of 5 mm the largest acceptable dimension of the scatterer might be less than 1 mm.

Of all the techniques using the principle of modulated scattering, the spinning-dipole technique [16] was most promising and we have extensively explored its possibilities in measuring EM fields in the frequency range of interest. Briefly, the technique employs the simplest possible scatterer, a short length of wire fixed to a thin nylon cord and spinning about an axis perpendicular to its length. The scatterer can easily be scaled down and its rate of spinning can be varied at will.

In practice, fixing the small dipole so that it is exactly perpendicular to the nylon cord is difficult. Further, incidental vibrations blur the exact position of the dipole, seriously affecting the performance of the spinning-dipole measuring system, particularly at shorter millimetric wavelengths. Vibrations of this nature greatly reduce the accuracy of field measurements due to unwanted phase changes in the scattered signal. These effects can be minimized by setting an upper limit to the rate of spinning. However, the modulating frequency is low and this imposes stringent requirements on the sensitivity and stability of the detection system.

Our efforts to eliminate spurious vibrations of the spinning dipole were not successful. We found it very much easier to dispense with spinning and simply to vibrate the dipole. The metallic dipole is now fixed longitudinally to the nylon cord which is made to vibrate so that the signal reradiated by the vibrating dipole is phase modulated and therefore easily distinguished from other background reflections.

Some features of the vibrating-dipole technique are worth noting. The dipole can be easily scaled down and alignment with the cord is also easy. Vibrations are stable, both frequency and amplitude being readily controlled. Smaller optimum amplitudes and higher vibration frequencies ease the requirements on the vibration and detection systems. Since the dipole vibrates in only one plane, the orthogonal field components, which are used to describe an arbitrarily polarized plane wave,

Manuscript received April 2, 1973; revised June 6, 1973.
The authors are with the Department of Electronics, University of Southampton, Southampton, England.

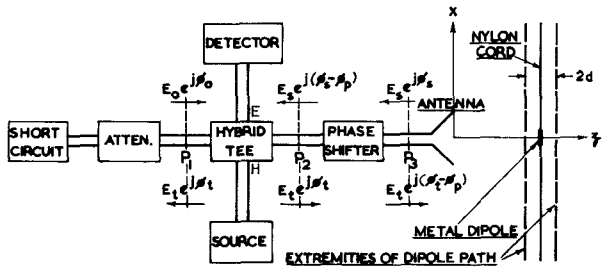

Fig. 1. Schematic of the apparatus basic to the vibrating-dipole technique.

may be measured both in amplitude and phase. It is perhaps relevant to note that the spinning-dipole technique [16] does not permit the measurement of fields other than those linearly polarized, without a previous knowledge of the polarization of the field with respect to the orientation of the dipole.

II. Principle of the Technique

Fig. 1 shows a schematic of the apparatus basic to the technique. A metallic dipole, in the form of a thin wire, is attached longitudinally to a nylon cord which vibrates in a plane. The perturbing dipole moves towards and away from the source and scatters the electric-field component parallel to its length, thus giving rise to a phase-modulated reflected wave. The reflected wave is combined with a reference wave in a hybrid T. The detected signal, at the vibration frequency of the perturbing dipole, contains information about the amplitude and phase of the EM field at the midpoint of the path of the vibrating dipole. By adjusting the phase shifter, relative amplitude and phase measurements of the EM field at various points in space are obtained. In addition, the orientation of the dipole in space provides information about the polarization of the EM wave.

III. Theory

In Fig. 1 it is assumed that the phase shifter and antenna are matched to the waveguide. An outgoing traveling wave whose complex amplitude at the center of the rectangular waveguide in the reference plane P_2 is denoted by $E_t \exp(j\phi_t)$, where E_t and ϕ_t are real quantities. At the reference plane P_3, this becomes $E_t \exp[j(\phi_t - \phi_p)]$, where ϕ_p rad is the phase lag due to the phase shifter. This wave will now produce an electric field $\boldsymbol{E}(x,y,z)$ in the free-space region outside the antenna.

The electric field $\boldsymbol{E}$ is clearly proportional to the incident wave $E_t \exp[j(\phi_t - \phi_p)]$ and therefore a normalized distribution function $\boldsymbol{F}$ can be defined through the relation

$$\boldsymbol{E}(x,y,z) = E_t \exp[j(\phi_t - \phi_p)]\boldsymbol{F}(x,y,z) \quad (1)$$

where $\boldsymbol{F}(x,y,z)$ is a dimensionless complex vector function of position and is now the quantity to be determined rather than $\boldsymbol{E}(x,y,z)$.

The perturbing dipole gives rise to a reflected wave whose complex amplitude at the reference plane P_3 shall be denoted by $E_s \exp(j\phi_s)$, where E_s and ϕ_s are real. An application of the Lorentz form of the reciprocity theorem [16] shows that the reflected wave is related to the incident wave via the relation[1]

$$E_s \exp(j\phi_s) = E_t \exp[j(\phi_t - \phi_p)]\left(\frac{j\omega\alpha Z_0}{ab}\right)(\hat{\boldsymbol{u}}\cdot\boldsymbol{F})^2 \quad (2)$$

where ω, α, and Z_0 are the angular frequency of the EM radiation, electric polarizability of the dipole, and characteristic impedance of the H_{10} mode in the rectangular waveguide, respectively. The waveguide dimensions are a and b and $\hat{\boldsymbol{u}}$ is the unit vector parallel to the dipole.

If the dipole is directed along the x axis and vibrates sinusoidally along the axis of propagation, i.e., the z axis, the product $\hat{\boldsymbol{u}}\cdot\boldsymbol{F}$ in (2) can be written as

$$\hat{\boldsymbol{u}}\cdot\boldsymbol{F} = F_x \exp[j(\phi_x + \phi_m \sin\omega_m t)] \quad (3)$$

where

$F_x \exp(j\phi_x)$ complex amplitude of the x-component of $\boldsymbol{F}$; F_x and ϕ_x correspond to amplitude and phase values (relative) of the x component of the electric field at the midpoint of the dipole's vibration;

ϕ_m $2\pi d/\lambda$, where $2d$ and λ are the peak-to-peak amplitude of vibration of the dipole and the free-space wavelength of radiation, respectively;

ω_m angular frequency of vibration of the dipole.

From (2) and (3) it follows that the complex amplitude of the reflected wave at the reference plane P_3 is

$$E_s \exp(j\phi_s) = \left(\frac{\omega\,|\,\alpha\,|\,Z_0E_t}{ab}\right)F_x^2 \cdot\exp[j(2\phi_x - \phi_p + 2\phi_m \sin\omega_m t + \phi_\alpha + \phi_t)] \quad (4)$$

where $|\,\alpha\,| \exp(j\phi_\alpha) = j\alpha$.

This reflected wave further passes through the phase shifter, and, on reaching the reference plane P_2, its complex amplitude will be

$$E_s \exp[j(\phi_s - \phi_p)] = \left(\frac{\omega\,|\,\alpha\,|\,Z_0E_t}{ab}\right)F_x^2 \cdot\exp[j\{2(\phi_x - \phi_p) + 2\phi_m \sin\omega_m t + \phi_\alpha + \phi_t\}]. \quad (5)$$

The complex amplitude of the reference wave entering the hybrid T, at the reference plane P_1, can be written as $E_0 \exp(j\phi_0)$, where E_0 and ϕ_0 are real. The phase angle ϕ_0 depends on the position of the short circuit and for simplicity we make $\phi_0 = \phi_\alpha + \phi_t$. Further, we can choose $\phi_t = -\phi_\alpha$ so that $\phi_0 = 0$.

The detector, which terminates the E arm of the hybrid T, responds to the phasor difference of the reference and reflected waves. Thus, assuming square-law detection,

[1] Equation (2) is the same as [16, eq. (42)] except for a slight change in notation.

the current through the detector is

$$\begin{aligned} i &= K \mid E_0 - E_s \exp\left[j\{2(\phi_x - \phi_p) + 2\phi_m \sin \omega_m t\}\right] \mid^2 \\ &= K\left[E_0^2 + E_s^2 - 2E_0E_sJ_0(2\phi_m) \cos 2(\phi_x - \phi_p)\right. \\ &\quad - 4E_0E_s \sum_{n=1}^{\infty} J_{2n}(2\phi_m) \cos 2(\phi_x - \phi_p) \cos 2n\omega_m t \\ &\quad \left. + 4E_0E_s \sum_{n=1}^{\infty} J_{2n-1}(2\phi_m) \sin 2(\phi_x - \phi_p) \sin (2n-1)\omega_m t\right] \end{aligned} \tag{6}$$

where K is a constant of proportionality of the detector,[2] and the J_n are Bessel functions of the first kind and integer order.

If a selective amplifier, into which the detector feeds, is tuned to the fundamental component ω_m, the rectified output is

$$V_0 = 4KGE_0E_sJ_1(2\phi_m) \mid \sin 2(\phi_x - \phi_p) \mid \tag{7}$$

where G is a constant due to amplification and rectification.

Substituting for E_s from (5),

$$V_0 = CF_x^2 \mid \sin 2(\phi_x - \phi_p) \mid \tag{8}$$

where C remains constant during measurement and is given by

$$C = \frac{4KGE_0E_t\omega \mid \alpha \mid Z_0J_1(2\phi_m)}{ab}. \tag{9}$$

From (8) it follows that relative measurements of the amplitude of the electric field in space can be determined by maximizing the rectified output with phase-shifter setting. Alternatively, relative phase measurements can be had by seeking a null in the rectified output.

It is interesting to note the dependence of the rectified output of the fundamental component on the amplitude of vibration of the dipole. In particular, an optimum output results when $2\phi_m = 4\pi d_{\text{opt}}/\lambda = 1.84$, for, at this value, the Bessel function $J_1(2\phi_m)$ is a maximum. The linear relation for optimum detection, i.e., $2d_{\text{opt}}/\lambda = 1.84/2\pi = 0.293$, further illustrates the suitability of the technique to the millimeter-wave region. As the wavelength decreases, smaller optimum amplitudes of vibration are needed, thus improving the mechanical stability and accuracy of the associated vibrating apparatus.

IV. Effect of Antenna Mismatch

So far it has been assumed that the phase shifter and antenna are matched to the waveguide. However, if the antenna is mismatched, the total received wave at the reference plane P_3 consists of an unmodulated component (due to the mismatch) in addition to the small phase-modulated component reflected by the vibrating dipole. Thus if $\rho \exp(j\phi)$ is the reflection coefficient at the reference plane P_3, looking towards the antenna and in the absence of the dipole, the complex amplitude of the unmodulated wave at P_3 is $\rho \exp(j\phi)E_t \exp\left[j(\phi_t - \phi_p)\right]$. This wave passes through the phase shifter and at the reference plane P_2 will be denoted by $E_u \exp\left[j2(\phi_u - \phi_p)\right]$, where $E_u = \rho E_t$ and $2\phi_u = \phi_t + \phi$. The detected current will now be given by

$$\begin{aligned} i' &= K \mid E_0 - E_u \exp\left[j2(\phi_u - \phi_p)\right] \\ &\quad - E_s \exp\left[j\{2(\phi_x - \phi_p) + 2\phi_m \sin \omega_m t\}\right] \mid^2 \\ &= K\left[E_0^2 + E_u^2 + E_s^2 - 2E_0E_u \cos 2(\phi_u - \phi_p)\right. \\ &\quad - 2E_0E_s \cos\{2(\phi_x - \phi_p) + 2\phi_m \sin \omega_m t\} \\ &\quad \left. + 2E_uE_s \cos\{2(\phi_x - \phi_u) + 2\phi_m \sin \omega_m t\}\right] \end{aligned} \tag{10}$$

and the amplified and rectified output of the fundamental component ω_m is

$$V_0' = CF_x^2 \left| \sin 2(\phi_x - \phi_p) - \left(\frac{E_u}{E_0}\right) \sin 2(\phi_x - \phi_u) \right| \tag{11}$$

where C is the constant defined by (9).

Equation (11) shows that errors in relative amplitude and phase measurements depend on ϕ_x, ϕ_u, and the ratio E_u/E_0. The presence of these types of error is easily observed by noting the variation in the rectified output with phase-shifter setting ϕ_p. The adjacent maxima in the rectified output differ by an amount depending on the value $2(E_u/E_0) \sin 2(\phi_x - \phi_u)$. One way to minimize the errors is to insert a matching device between the phase shifter and antenna. With good matching, equal maxima of the rectified output are observed as the phase shifter is altered. In practice, this degree of matching is difficult to achieve and is sensitive to slight changes in the source frequency. The residual VSWR for a particular ratio of E_u/E_0 is given by

$$\begin{aligned} S = \frac{1+\rho}{1-\rho} &= \frac{1 + E_u/E_t}{1 - E_u/E_t} \\ &= \frac{1 + (E_u/E_0)(E_0/E_t)}{1 - (E_u/E_0)(E_0/E_t)}. \end{aligned} \tag{12}$$

The level of E_0 must be appropriate for proper detection, whereas that of E_t, which is directly related to the transmitted power, can be as high as possible. A typical value of E_0/E_t might be 0.1. Thus, in order to achieve a ratio of E_u/E_0 better than 0.1 (corresponding to ± 10-percent error in amplitude measurement and $\pm 3°$ in phase measurement), the residual VSWR must be less than 1.02.

V. Coherent Detection System

An alternative and more elegant approach to the problem of antenna mismatch is to use a coherent detection system [11]. In its simplest form this is achieved by modifying the arrangement in Fig. 1 in the following way: the short circuit and detector are removed from the

[2] It should be noted that it is not essential for the detector to have a square-law characteristic. Provided $E_0 \gg E_s$, any arbitrary functional relationship will give a result similar to (6).

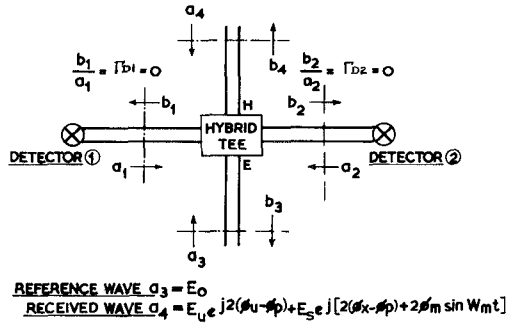

Fig. 2. Schematic of the detector hybrid T.

"transmit–receive" hybrid T, and the reference and received waves are now fed to the E and H arms, respectively, of another hybrid T. The symmetrical arms of this "detector" hybrid T are terminated with a pair of detecting elements and their outputs subtracted. If the detector hybrid T is perfect and the detecting elements identical, the rectified output of the fundamental component ω_m from the coherent detection system is that in (7). Thus there are no errors in amplitude and phase measurements due to the unmodulated component of received waves [11].

In practice the hybrid T is not ideal and the detectors not identical. Fig. 2 shows the detector hybrid T with the reference and received waves in the terminal planes. It is assumed that all four ports connecting the hybrid T are matched.

The hybrid T is regarded as a lossless reciprocal 4-port and hence

$$\begin{bmatrix} b_1 \\ b_2 \\ b_3 \\ b_4 \end{bmatrix} = \begin{bmatrix} S_{11} & S_{12} & S_{13} & S_{14} \\ S_{12} & S_{22} & S_{23} & S_{24} \\ S_{13} & S_{23} & S_{33} & S_{34} \\ S_{14} & S_{24} & S_{34} & S_{44} \end{bmatrix} \begin{bmatrix} 0 \\ 0 \\ a_3 \\ a_4 \end{bmatrix} \tag{13}$$

where S_{ij} is an element of the scattering matrix of the hybrid T.

Because we are only interested in the waves incident on the detectors,

$$\begin{aligned} b_1 &= S_{13}a_3 + S_{14}a_4 \\ b_2 &= S_{23}a_3 + S_{24}a_4. \end{aligned} \tag{14}$$

The elements of the scattering matrix are complex, and hence (14) may be written

$$\begin{aligned} b_1 &= \exp(j\phi_{13})[\,|\,S_{13}\,|\,a_3 + |\,S_{14}\,|\exp[\,j(\phi_{14} - \phi_{13})\,]a_4] \\ b_2 &= \exp(j\phi_{23})[\,|\,S_{23}\,|\,a_3 + |\,S_{24}\,|\exp[\,j(\phi_{24} - \phi_{23})\,]a_4]. \end{aligned} \tag{15}$$

We can choose the reference planes so that $\phi_{14} - \phi_{13} = 0$. Further, we define $\phi_e = \phi_{24} - \phi_{23}$.

Now, assuming square-law detectors, the detected currents are

$$i_1 = K_1 |\,b_1\,|^2 = K_1 \big|\,|\,S_{13}\,|\,a_3 + |\,S_{14}\,|\,a_4\,\big|^2 \tag{16}$$

$$i_2 = K_2 |\,b_2\,|^2 = K_2 \big|\,|\,S_{23}\,|\,a_3 + |\,S_{24}\,|\,e^{j\phi_e}a_4\,\big|^2 \tag{17}$$

where K_1 and K_2 are proportionality constants depending on the characteristics of the detectors.

On substituting $a_3 = E_0$,

$$\begin{aligned} a_4 &= E_u \exp[\,j2(\phi_u - \phi_p)\,] \\ &\quad + E_s \exp[\,j\{2(\phi_x - \phi_p) + 2\phi_m \sin \omega_m t\}\,] \\ i_1 &= K_1 \big|\,|\,S_{13}\,|\,E_0 + |\,S_{14}\,|\,E_u \exp[\,j2(\phi_u - \phi_p)\,] \\ &\quad + |\,S_{14}\,|\,E_s \exp[\,j\{2(\phi_x - \phi_p) + 2\phi_m \sin \omega_m t\}\,]\,\big|^2 \\ &= K_1[\,|\,S_{13}\,|^2 E_0^2 + |\,S_{14}\,|^2 E_u^2 + |\,S_{14}\,|^2 \\ &\quad + 2\,|\,S_{13}\,|\,|\,S_{14}\,|\,E_0E_u \cos 2(\phi_u - \phi_p) \\ &\quad + 2\,|\,S_{13}\,|\,|\,S_{14}\,|\,E_0E_s \\ &\quad \cdot \cos\{2(\phi_x - \phi_p) + 2\phi_m \sin \omega_m t\} + 2\,|\,S_{14}\,|^2 E_uE_s \\ &\quad \cdot \cos\{2(\phi_x - \phi_u) + 2\phi_m \sin \omega_m t\}\,] \end{aligned} \tag{18}$$

and

$$\begin{aligned} i_2 &= K_2 \big|\,|\,S_{23}\,|\,E_0 + |\,S_{24}\,|\,E_u \exp[\,j\{2(\phi_u - \phi_p) + \phi_e\}\,] \\ &\quad + |\,S_{24}\,|\,E_s \exp[\,j\{2(\phi_x - \phi_p) + 2\phi_m \sin \omega_m t + \phi_e\}\,]\,\big|^2 \\ &= K_2[\,|\,S_{23}\,|^2 E_0^2 + |\,S_{24}\,|^2 E_u^2 + |\,S_{24}\,|^2 E_s^2 \\ &\quad + 2\,|\,S_{23}\,|\,|\,S_{24}\,|\,E_0E_u \cos\{2(\phi_u - \phi_p) + \phi_e\} \\ &\quad + 2\,|\,S_{23}\,|\,|\,S_{24}\,|\,E_0E_s \\ &\quad \cdot \cos\{2(\phi_x - \phi_p) + 2\phi_m \sin \omega_m t + \phi_e\} \\ &\quad + 2\,|\,S_{24}\,|^2 E_uE_s \cos\{2(\phi_x - \phi_u) + 2\phi_m \sin \omega_m t\}\,]. \end{aligned} \tag{19}$$

Thus the amplified and rectified output of the fundamental component ω_m from the coherent detection (OCD) system is

$$\begin{aligned} V_{OCD} &= G\,|\,(i_1 - i_2)\omega_m\,| \\ &= 4GE_0E_sJ_1(2\phi_m) \Big|K_1\,|\,S_{13}\,|\,|\,S_{14}\,|\sin 2(\phi_x - \phi_p) \\ &\quad - K_2\,|\,S_{23}\,|\,|\,S_{24}\,|\sin\{2(\phi_x - \phi_p) + \phi_e\} \\ &\quad + (K_1\,|\,S_{14}\,|^2 - K_2\,|\,S_{24}\,|^2)\left(\frac{E_u}{E_0}\right)\sin 2(\phi_x - \phi_u)\Big| \\ &= P\Big|\sin\{2(\phi_x - \phi_p) - \phi_r\} \\ &\quad + Q\left(\frac{E_u}{E_0}\right)\sin 2(\phi_x - \phi_u)\Big| \end{aligned} \tag{20}$$

where

$$P = 4GE_0E_sJ_1(2\phi_m)\,(K_1^2 \mid S_{13}\mid^2 \mid S_{14}\mid^2 + K_2^2 \mid S_{23}\mid^2 \mid S_{24}\mid^2 - 2K_1K_2 \mid S_{13}\mid \mid S_{14}\mid \mid S_{23}\mid \mid S_{24}\mid \cos\phi_e)^{1/2} \quad (21)$$

$$\phi_r = \tan^{-1}\left\{\frac{K_2 \mid S_{23}\mid \mid S_{24}\mid \sin\phi_e}{K_1 \mid S_{13}\mid \mid S_{14}\mid - K_2 \mid S_{23}\mid \mid S_{24}\mid \cos\phi_e}\right\} \quad (22)$$

$$Q = \frac{K_1 \mid S_{14}\mid^2 - K_2 \mid S_{24}\mid^2}{(K_1^2 \mid S_{13}\mid^2 \mid S_{14}\mid^2 + K_2^2 \mid S_{23}\mid^2 \mid S_{24}\mid^2 - 2K_1K_2 \mid S_{13}\mid \mid S_{14}\mid \mid S_{23}\mid \mid S_{24}\mid \cos\phi_e)^{1/2}}. \quad (23)$$

Equation (20) is similar in form to (11) and therefore the measured amplitude and phase are still affected by the amplitude and phase of the unmodulated wave $E_u \exp[j2(\phi_u - \phi_p)]$. As before, the presence of these errors is easily observed by noting the variation of the rectified output with the setting of the phase shifter; the adjacent maxima in the output differ by an amount depending on $Q(E_u/E_0)\sin 2(\phi_x - \phi_u)$. This effect can be minimized by matching the antenna to the waveguide. However, there is a limit to the degree of matching that can be achieved in practice. An alternative method of minimizing the effect of an unmodulated wave is to amplify the signals from the two detectors separately before subtraction takes place. Thus, if G_1 and G_2 are the gains of the amplifiers following detectors ① and ②, the rectified fundamental component of the output from the coherent detection system is

$$V_{OCD}' = P'\left|\sin\{2(\phi_x - \phi_p) - \phi_r'\} + Q'\left(\frac{E_u}{E_0}\right)\sin 2(\phi_x - \phi_u)\right| \quad (24)$$

where the primes are used to distinguish this arrangement from that using common amplification, and

$$P' = 4E_0E_sJ_1(2\phi_m)\,(G_1^2K_1^2 \mid S_{13}\mid^2 \mid S_{14}\mid^2 + G_2^2K_2^2 \mid S_{23}\mid^2 \mid S_{24}\mid^2 - 2K_1K_2G_1G_2 \mid S_{13}\mid \mid S_{14}\mid \mid S_{23}\mid \mid S_{24}\mid \cos\phi_e)^{1/2} \quad (25)$$

$$\phi_r' = \tan^{-1}\left\{\frac{G_2K_2 \mid S_{23}\mid \mid S_{24}\mid \sin\phi_e}{G_1K_1 \mid S_{13}\mid \mid S_{14}\mid - G_2K_2 \mid S_{23}\mid \mid S_{24}\mid \cos\phi_e}\right\} \quad (26)$$

$$Q^1 = \frac{G_1K_1 \mid S_{14}\mid^2 - G_2K_2 \mid S_{24}\mid^2}{(G_1^2K_1^2 \mid S_{13}\mid^2 \mid S_{14}\mid^2 + G_2^2K_2^2 \mid S_{23}\mid^2 \mid S_{24}\mid^2 - 2K_1K_2G_1G_2 \mid S_{13}\mid \mid S_{14}\mid \mid S_{23}\mid \mid S_{24}\mid \cos\phi_e)^{1/2}}. \quad (27)$$

If G_1 and G_2 are adjusted so that $G_1K_1 \mid S_{14}\mid^2 - G_2K_2 \mid S_{24}\mid^2 = 0$, then from (27) $Q' = 0$, and the rectified output, as given by (24), is free from errors which are introduced by the unmodulated received wave. In practice, the amplifier gains, G_1 and G_2, are adjusted until the maxima of the rectified output are equal and not affected by the setting of the phase shifter. Thus the output of the coherent detection system with a correct equalization is independent of the amplitude and phase of the unmodulated component of received wave. This is valid provided the unmodulated received wave is small compared to the reference wave, and follows from the fact that the self-bias levels of the two detectors are affected by the amplitude and phase of the unmodulated wave in differing ways [see (18) and (19)]. Hence the assumption that the detector characteristics remain constant for all power levels is not strictly true. In practice, matching of the antenna, followed by the adjustment of the amplifier gains, ensures operation free from adverse effects of the unmodulated wave.

VI. Mismatch of the Phase Shifter and Drift in Source Frequency

Microwave phase shifters are calibrated under matched conditions. When a phase shifter is mismatched the phase-shift indication differs from that given by the calibration curve. In the vibrating-dipole technique, the phase shifter is matched to the antenna when equal maxima in the detected output are observed as the phase shifter is altered. Matching the other port of the phase shifter is achieved by means of a tuner which is adjusted so that successive nulls in the detected output are obtained by altering the phase shifter by 90°. It has been shown previously that the detected output is of the form $\mid \sin\{2(\phi_x - \phi_p) - \phi_r'\}\mid$ where ϕ_r' is a constant, ϕ_p is the phase-shifter setting, and ϕ_x is the phase of the EM field.

The accuracy of phase measurements in our technique, in common with other homodyne bridge techniques, is affected by the drift in the source frequency if the electrical lengths of the two arms of the bridge are not equal. This error can be minimized by adding lengths of waveguide to the shorter path. However, the signal path changes as the dipole is moved to different locations in space; therefore, true equalization of path lengths is not always possible. In practice, this is not a serious problem because the change in signal path length during a particular set of measurements seldom exceeds a few wavelengths in free space.

VII. Misalignment Between the Line of Dipole Vibration and the Direction of the Wave

The theory of the technique given in Section III assumes that the dipole vibrates sinusoidally along the axis of propagation. However, if the direction of wave propagation is inclined at an angle θ to the line of vibra-

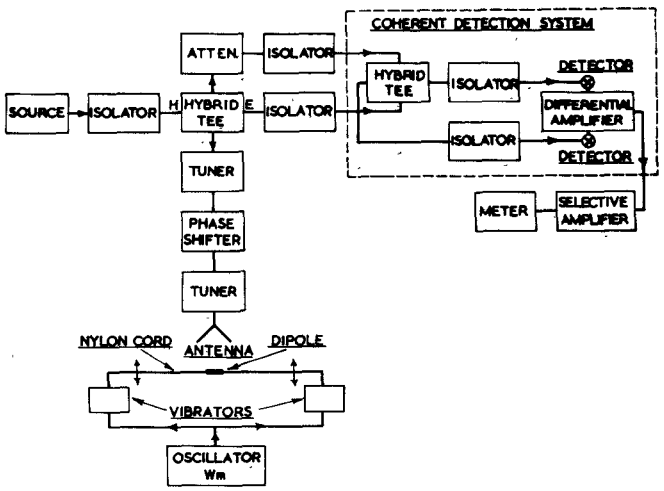

Fig. 3. Block diagram of the experimental equipment for measuring EM fields by the vibrating-dipole technique.

tion, the index of phase modulation of the wave reflected from the dipole depends not only on the amplitude of vibration but also on the angle of inclination. The index of phase modulation is now given by $2\phi_m = (4\pi d \cos\theta)/\lambda$ and the fundamental component of the detected signal is affected by it via the $J_1(2\phi_m)$ term [see (8) and (9)]. It is evident that errors in relative amplitude measurements of the field will arise if the angle of inclination varies with the location of the dipole.

A radiating aperture, when viewed in the far field, can be considered as a point source with spherical wavefronts. Therefore, relative amplitude measurements of the far field taken in a Cartesian plane, with the dipole always vibrating along a line normal to this plane, will be in error. These errors can be eliminated by adjusting the amplitude of vibration so that a maximum in the detected output always results. This occurs when $J_1(2\phi_m)$ is a maximum or $2\phi_m = 1.84$. In practice, very little adjustment is necessary if the amplitude of vibration is initially set for a maximum in the detected output. The shape of the function $J_1(2\phi_m)$ corresponding to this region of operation is fairly insensitive to changes in the argument $2\phi_m$ and hence to changes in the angle of inclination.

VIII. Apparatus

A block schematic of the apparatus used in the vibrating-dipole technique of field measurement is shown in Fig. 3.

RG98/U waveguide components are used throughout and the source is a reflex klystron giving 200 mW over the 62.3–62.8-GHz range. The source power is fed into the H arm of a transmit–receive hybrid T. One of the collinear arms of the hybrid T feeds, via an attenuator, into the E-arm of the detector hybrid T and provides the reference signal to the coherent detection system. The other collinear arm contains a calibrated phase shifter with E/H tuners on either side, and an antenna radiating into space. The phase-modulated signal, reradiated by the vibrating dipole, is picked up by the same antenna and enters the transmit–receive hybrid T. The signal emerging from the E-arm of this hybrid T then feeds directly into the H-arm of the detector hybrid T where it mixes with the reference signal in the detecting elements in the two collinear arms. It is worth pointing out that a circulator could replace a hybrid T to perform the transmit–receive operation. The reference signal would then be obtained via a directional coupler placed in the main transmission path. This arrangement makes a better use of source power, but was not used because a circulator was not available at the time our measurements were taken.

The signals from the two detectors feed into a differential amplifier having separate gain controls for each channel. The output from the differential amplifier is then fed into a selective amplifier tuned to the dipole vibration frequency. A moving-coil meter is connected across the output terminals of the selective amplifier.

The apparatus for supporting and vibrating the dipole consists of a circular Paxolin frame, 70-cm internal diameter, which itself is mounted on ball bearings on to a rigid metal frame. Two small vibrators are mounted diametrically opposite to each other on the circular frame. A nylon cord of diameter 0.005 in is threaded through small holes in the driving spindles of each vibrator, and is then fixed at both ends to tensioning supports. The metal dipole is glued to the nylon cord, care being taken that it is truly parallel to the cord. Rotation of the circular frame together with the vibrating dipole enables any transverse component of the EM field to be measured.

The size of the dipole depends on the region of the EM field in which measurements are to be made. For measurements in the far-field region, given in Section IX, the dipole used is about a half-wavelength long to give maximum response of the detected signal.

A most convenient way of positioning the dipole in the field is to mount the waveguide equipment on an adjustable table. The dipole-supporting frame is kept fixed while the antenna and waveguide equipment is moved in three dimensions. This arrangement is convenient because waveguide components at millimetric wavelengths are small.

The adjustable table consists of a bracket mounted on three pairs of steel rods, 3/4 in in diameter, machined to an accuracy of 0.0005 in. Each pair of rods is perpendicular to the other two, thus allowing movement of the bracket in three mutually perpendicular directions. The bracket can move 30 cm in the vertical plane and 20 cm in the horizontal plane. Calibrated dial gauges, mounted in appropriate positions, are used to measure the displacement of the bracket in any of the three directions to within 0.01 mm.

The whole apparatus is arranged so that the antenna is directed towards a region in the room which is clear of unwanted obstacles. The dipole-supporting frame is sufficiently large to be clear of the main lobe of the radiating antenna. Thus unwanted reflections which might distort the field at the dipole are kept to a minimum.

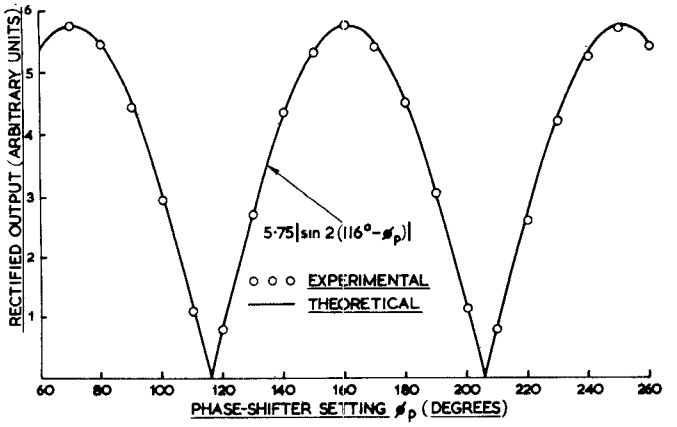

Fig. 4. Dependence of the rectified output on the phase-shifter setting.

IX. Experimental Results

The following experiments were performed to demonstrate the feasibility and accuracy of the technique in the measurement of millimeter-wave fields. In all measurements $\lambda = 4.80$ mm and the frequency of vibration $\omega_m/2\pi = 180$ Hz. The dipole was a straight piece of SWG 45 copper wire, 2.1 mm in length.

A. Dependence of Rectified Output on the Phase-Shifter Setting

It is shown in Section V that the rectified output of the fundamental component, from the coherent detection system with proper equalization, is of the form

$$V_{OCD}' = P' \mid \sin \{2(\phi_X - \phi_p) - \phi_r'\} \mid \qquad (28)$$

where P' and ϕ_r' are constants and ϕ_p is the setting of the phase shifter.

An experiment was carried out to verify this relationship. The dipole was located in the far field of a small pyramidal horn. Adjustment to the gains of the two channels of the differential amplifier and matching of the horn, as outlined in Section V, were carried out.

The experimental points in Fig. 4 give the measured dependence of the rectified output with the setting. The good agreement with the theoretical curve indicates that matching of the horn and phase shifter, and correct adjustment of the differential amplifier have been achieved. Thus, in subsequent field measurements, errors due to leakage of an unmodulated wave are considered to be negligible.

B. Relative Amplitude Measurements

Relative amplitude measurements of the x component of the electric field were taken in the far field of a small pyramidal horn, along the axis of propagation.

If the amplitude of the electric field at a distance z_0 is denoted by $E_x(z_0)$ then at $z_0 + \delta z$, the amplitude is

$$E_x(z_0 + \delta z) = \left(\frac{r_0}{r_0 + \delta z}\right) E_x(z_0) \qquad (29)$$

where r_0 is the distance between the initial rest position of the dipole and the location of the apparent point source of the horn.

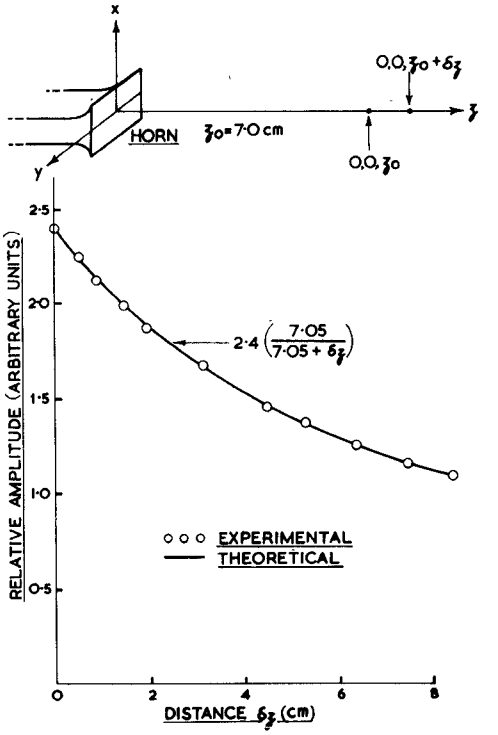

Fig. 5. Amplitude distribution in the far field of a pyramidal horn.

Fig. 5 illustrates the variation in the relative amplitude of the electric field with incremental distance from the apparent point source. A good fit of (29) to the measured data is obtained when $r_0 = 7.05$ cm. All the experimental points are very close to the theoretical curve and show that the effect of background reflections on the incident field is negligible.

C. Relative Phase Measurements

Relative phase measurements of the x component of the electric field were taken in the far field of the horn along the path $x = 0$, y, $z = 7.0$ cm (Fig. 6). Assuming the horn to be a point source, the phase variation relative to the point $x = 0$, $y = 0$, $z = 7.0$ cm is

$$\Delta\phi_x = \frac{360}{\lambda}[(s_0^2 + y^2)^{1/2} - s_0] \text{ deg (lag)} \qquad (30)$$

where the wavelength $\lambda = 4.8$ mm and s_0 is the distance of the initial rest position of the dipole to the phase center of the apparent point source. The theoretical and measured data given in Fig. 6 agree well when $s_0 = 7.10$ cm.

X. Conclusions

A technique has been developed for measuring amplitude and phase distributions of EM fields at millimetric wavelengths. The validity of the method has been verified and the accuracy demonstrated by measurements at 62.5 GHz. In particular, the amplitude and phase were measured in the far field of a linearly polarized radiator,

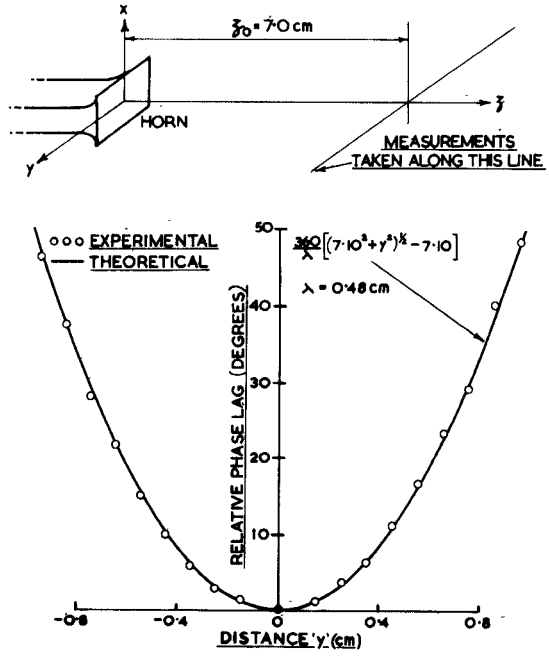

Fig. 6. Phase distribution in the far field of a pyramidal horn.

for which theoretical field-distribution curves are available.

The technique, in common with some other methods of EM field measurement, makes use of a coherent detection system. The advantages of coherent detection are that it eases requirements imposed on some components of the microwave circuit and eliminates the effects due to unmodulated backscatter.

A detailed error analysis has been performed and procedures for minimizing the errors have been established. The accuracy of EM field determination is virtually independent of frequency except that, at very short millimetric wavelengths, it is limited by the mechanical tolerances of the small waveguide components. In particular, the accuracy of measurement depends on the precision of the phase shifter. In our experiments the phase was measured to an accuracy of 2°.

The vibrating-dipole technique differs from other field measuring techniques in that it employs a modulated scatterer of great versatility and simplicity. The vibrating dipole is made of wire and is fixed longitudinally to a thin nylon cord. The frequency, amplitude, and plane of vibration can be easily changed and adjusted during the test while the dipole itself can be easily scaled up or down.

Although we have stressed its applicability to millimetric wavelengths, the vibrating-dipole technique can be employed over the whole microwave spectrum (bands 10 and 11). However, its advantages become particularly important at millimetric wavelengths. So far as we are aware, no other technique can produce, at millimetric wavelengths, observations of comparable accuracy of amplitude and phase distributions of EM fields.

Some modifications subsequently introduced and some preliminary tests indicate that the vibrating-dipole technique lends itself to: 1) measurement of near-field distributions; 2) simultaneous display of amplitude and phase; 3) automatic field plotting; and 4) measurement of arbitrarily polarized fields.

References

[1] R. D. Kodis, "Diffraction measurements at 1.25 centimetres," *J. Appl. Phys.*, vol. 23, pp. 249–255, Feb. 1952.
[2] M. J. Ehrlich *et al.*, "Studies of the diffraction of electromagnetic waves by circular apertures and complementary obstacles: The near-zone field," *J. Appl. Phys.*, vol. 26, pp. 336–345, Mar. 1955.
[3] R. M. Barrett and M. H. Barnes, "Automatic antenna wavefront plotter," *Electronics*, vol. 25, pp. 120–125, Jan. 1952.
[4] J. Bacon, "An *X*-band phase plotter," in *Proc. Nat. Electronics Conf.*, vol. 10, pp. 256–263, Oct. 1954.
[5] O. J. H. Harries, "Cavity resonators and electron beams," *Wireless Eng.*, vol. 24, pp. 135–144, May 1947
[6] L. C. Maier and J. C. Slater, "Field strength measurements in resonant cavities," *J. Appl. Phys.*, vol. 23, pp. 68–76, Jan. 1952.
[7] L. C. Maier and J. C. Slater, "Determination of field strength in a linear accelerator cavity," *J. Appl. Phys.*, vol. 23, pp. 78–83, Jan. 1952.
[8] T. Morawski, "Application of the perturbation method in some microwave measurements," *IEEE Trans. Instrum. Meas.*, vol. IM-19, pp. 373–376, Nov. 1970.
[9] R. Justice and V. H. Rumsey, "Measurement of electric field distributions," *IRE Trans. Antennas Propagat.*, vol. AP-3, pp. 177–180, Oct. 1955.
[10] R. H. Miller, "A linear electron accelerator for submillimeter wave generation," Microwave Lab., Stanford Univ., Stanford, Calif., Rep. 1244, pp. 57–70, Oct. 1964.
[11] J. H. Richmond, "A modulated scattering technique for measurement of field distributions," *IRE Trans. Microwave Theory Tech.*, vol. MTT-3, pp. 13–15, July 1955.
[12] B. J. Strait and D. K. Cheng, "Microwave magnetic-field measurements by a modulated scattering technique," *Proc. Inst. Elec. Eng.*, vol. 109B, pp. 33–39, Jan. 1962.
[13] A. Vural, D. K. Cheng, and B. J. Strait, "Measurement of diffraction fields of finite cones by a scattering technique using light modulation," *IEEE Trans. Antennas Propagat.*, vol. AP-11, pp. 200–201, Mar. 1963.
[14] T. Toyonaga, "Antennas for measurement of microwave electromagnetic field by a light-modulated scattering technique," *Electron. Commun. Japan*, vol. 54-B, 1971.
[15] K. Iizuka, "Photoconductive probe for measuring electromagnetic fields," *Proc. Inst. Elec. Eng.*, vol. 100, pp. 1747–1754, Oct. 1963.
[16] A. L. Cullen and J. C. Parr, "A new perturbation method for measuring microwave fields in free-space," *Proc. Inst. Elec. Eng.*, vol. 106B, pp. 836–844, Nov. 1955.
[17] K. Iizuka, "A new technique for measuring an electromagnetic field by a coil spring," *IEEE Trans. Microwave Theory Tech.*, vol. MTT-11, pp. 498–505, Nov. 1963.